Journal of Magnetism and Magnetic Materials 371 (2014) 77–81

Contents lists available at ScienceDirect

Journal of Magnetism and Magnetic Materials

journal homepage: www.elsevier.com/locate/jmmm

Quantum phase transition and thermodynamic properties of a fourfold magnetic periodic system

Shuling Wang [a], Ruixue Li [a], Linjie Ding [b], Hua-Hua Fu [a], Si-cong Zhu [a], Yun Ni [c], Yan Meng [d], Kailun Yao [a,e,*]

[a] School of Physics and Wuhan National High Magnetic Field Center, Huazhong University of Science and Technology, Wuhan 430074, China
[b] Department of Physics, China Three Gorges University, Yi Chang 443002, China
[c] Huazhong University of Science and Technology, Wenhua College, Wuhan 430074, China
[d] Department of Physics, Xingtai University, Xingtai 054001, China
[e] International Center of Materials Physics, Chinese Academy of Science, Shenyang 110015, China

ARTICLE INFO

Article history:
Received 21 March 2014
Received in revised form
25 June 2014
Available online 24 July 2014

Keywords:
Thermodynamic
Magnetization plateau
Energy spectra

ABSTRACT

Based on the experimental synthesis of organic compound verdazyl radical β-3-(2,6-dichlorophenyl)-1,5-diphenylverdazyl, consisting of four antiferromagnetic couplings, we study the magnetic properties and thermodynamic behaviors for different antiferromagnetic interactions using Green's function theory. Under different fields, there are five regimes containing two gapless phases and three magnetization plateaus ($M=0$, 1/2 and saturated magnetization) distinguished by four critical lines, which are evidenced by the two-site entanglement entropy and closely related to the energy spectra. In addition, we calculate the susceptibility and specific heat, to demonstrate the low-lying excitations at low temperatures. It will provide guidance for us to synthesize varieties of unconventional magnetic materials, and stimulate future studies on quantum spin systems.

1. Introduction

Low-dimensional quantum spin systems are an attractive field in condensed matter physics in the past decades. In particular, the $S=1/2$ Heisenberg antiferromagnetic chain (HAFC) has been intensively investigated in strongly correlated quantum many-body systems, because it is one of the simple quantum spin systems that can be used to simulate various quantum behavior of a wide range of materials.

Among them, the bond alternating chain (BAC) has been widely studied both theoretically [1–8] and experimentally [9–12]. Manaka and Yamada [9] reported that the $S=1/2$ compound $(CH_3)CHNH_3CuCl_3$ (IPACuCl$_3$) was ferromagnetic (F)- antiferromagnetic (AF) alternating chain with an energy gap in terms of Haldane conjecture [13]. In addition, the magnetic properties such as the magnetization, the susceptibility and the specific heat of BAC with period $n=3$ (AF-AF-F and F-F-AF) were also studied by Gu et al. [4]. There was another BAC with fourfold magnetic periodicity, which consists of AF-AF-F-F [6,12], AF$_1$-AF$_2$-AF$_1$-F [7,8], and F-AF$_1$-F-AF$_2$ [14]. In such system, there is a gap, corresponding to the excitation from the singlet ground state to the triplet excited state without magnetic field. In 2013, Yamaguchi et al. [15] have synthesized a single crystal of the verdazyl radical β-3-(2,6-dichlorophenyl)-1,5-diphenylverdazyl and analyzed its crystal structure, which can be described as a spin $S=1/2$ tetrameric HAFC with AF$_1$-AF$_2$-AF$_3$-AF$_2$ interactions. Meanwhile, they also observed that the modulation of magnetic interaction can be realized by using chemical modification [16]. The magnetic susceptibility, magnetization curves and specific heat have been successfully explained. In order to further explore the quantum nature of magnetization plateaus and the phase diagram, the quantum phase transition and thermodynamics for different antiferromagnetic couplings will be studied in this paper. It will provide guidance for us to synthesize a variety of unconventional magnetic materials, and stimulate future studies on quantum spin systems.

2. Model and Hamiltonian

From the structure of verdazyl radical β-3-(2,6-dichlorophenyl)-1,5-diphenylverdazyl (β−2,6−Cl$_2$−V) illustrated in Fig. 1 of Ref. [15], there are three types of dominating interaction J_1, J_2 and J_3, respectively. The spin Hamiltonian reads

$$H=\sum_i[J_1\vec{S}_{4i+1}\cdot\vec{S}_{4i+2}+J_2\vec{S}_{4i+2}\cdot\vec{S}_{4i+3}+J_3\vec{S}_{4i+3}\cdot\vec{S}_{4i+4}+J_2\vec{S}_{4i}\cdot\vec{S}_{4i+1})_\Delta-h(S^z_{4i+1}+S^z_{4i+2}+S^z_{4i+3}+S^z_{4i+4})] \quad (1)$$

* Corresponding author.
E-mail addresses: wangshuling0324.student@sina.com, slwang2010@hust.edu.cn (S. Wang).

http://dx.doi.org/10.1016/j.jmmm.2014.07.034
0304-8853/

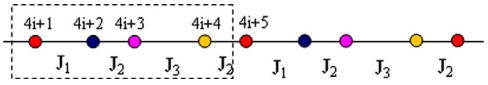

Fig. 1. Sketch of the tetrameric structure of $\beta-2,6-Cl_2-V$ along the a axis. The solid circles represent spin-1/2. The dashed rectangle is magnetic unit cell.

where $J_i>0$ $(i=1, 2, 3)$ are antiferroagnetic couplings between the nearest spins along the chain and $(\vec{S}_i\cdot\vec{S}_j)_\Delta = S_i^xS_j^x+S_i^yS_j^y+\eta S_i^zS_j^z$ with η denoting the anisotropy, $h=g\mu_BB$ is defined as the reduced magnetic field.

By performing the Jordan–Wigner (JW) transformation [17–19], the Hamiltonian (1) becomes

$$\begin{aligned}H=\sum_i\Big[&\frac{1}{2}(J_1a_i^+b_i+J_2b_i^+c_i+J_3c_i^+d_i+J_2d_{i-1}^+a_i+h.c.)\\&+J_1\left(a_i^+a_i-\frac{1}{2}\right)\left(b_i^+b_i-\frac{1}{2}\right)+J_2\left(b_i^+b_i-\frac{1}{2}\right)\left(c_i^+c_i-\frac{1}{2}\right)\\&+J_3\left(c_i^+c_i-\frac{1}{2}\right)\left(d_i^+d_i-\frac{1}{2}\right)+J_2\left(d_{i-1}^+d_{i-1}-\frac{1}{2}\right)\left(a_i^+a_i-\frac{1}{2}\right)\\&-h(a_i^+a_i+b_i^+b_i+c_i^+c_i+d_i^+d_i-2)\Big]\end{aligned}\tag{2}$$

We would like to mention that the phase transitions are signaled by the two-site entanglement entropy [20,21]

$$S_{ij}=-Tr[\rho_{ij}\ln(\rho_{ij})]\tag{3}$$

wherein ρ_{ij}, consisting of correlation functions, is the two-site reduced density matrix of the system at site i and j. Herein, we define the two-site entanglement entropy S_{41} connected by J_2 between cells, and $S_{12,}$ S_{23}, and S_{34} connected by J_1, J_2 and J_3 inside the cell, respectively.

To calculate the correlation functions, and perform magnetic and thermodynamic properties, we employ the equations of motion method of retarded Green's function [22,23], which is described as

$$G_{ij}(t-t')=\ll a_i(t);b_j^+(t')\gg=-i\theta(t-t')\left\langle a_ib_j^++b_j^+a_i\right\rangle\tag{4}$$

where the subscripts i and j label lattice sites. After the time Fourier transformation, the Green's function is put into the equation of motion,

$$\omega\ll a_i;b_j^+\gg=\left\langle[a_i;b_j^+]_+\right\rangle+\ll[a_i,H];b_j^+\gg\tag{5}$$

For the term $\ll[a_i,H];b_j^+\gg$ of Eq. (5), by using a similar equation of motion as Eq. (5), it will make the higher-order Green's function appearing, giving rise to an infinite set of coupled equations. By using bond-mean-field theory (BMFT), we adopt the decoupling scheme [24] for Ising quartic term in Eq. (5)

$$\begin{aligned}\alpha_i^+\alpha_i\alpha_{i+1}^+\alpha_{i+1}\approx&\langle\alpha_i\alpha_{i+1}^+\rangle\alpha_i^+\alpha_{i+1}+\langle\alpha_{i+1}\alpha_i^+\rangle\alpha_{i+1}^+\alpha_i\\&+\langle\alpha_i\alpha_{i+1}^+\rangle\langle\alpha_{i+1}\alpha_i^+\rangle,(\alpha=a,b,c,d)\end{aligned}\tag{6}$$

For further Fourier transformation into momentum space, the Green's function can be expressed as

$$G_{ij}=\frac{1}{N}\sum_k g(k)e^{ik(i-j)}\tag{7}$$

The integral of the wave vector k is along the chain direction. So, the momentum space Green's function $g(k,\omega)$ can be characterized as a function of wave vector k and the elementary excitation spectrum $\omega=\omega(k)$.

According to the standard spectral theorem, the correlation function of the fermion operators can be obtained by

$$\left\langle b_j^+a_i\right\rangle=\frac{i}{2\pi N}\sum_k e^{ik(i-j)}\int\frac{d\omega}{e^{\beta\omega}+1}[g(k,\omega+i0^+)-g(k,\omega-i0^+)]\tag{8}$$

where $\beta=1/k_BT$, k_B and T are the Boltzmann's constant and the absolute temperature, respectively.

Then, the average magnetization M per cell and magnetic susceptibility χ can be described as

$$M=\frac{1}{N}\sum_i\left(\langle S_{4i+1}^z\rangle+\langle S_{4i+2}^z\rangle+\langle S_{4i+3}^z\rangle+\langle S_{4i+4}^z\rangle\right),\ \chi=\frac{\partial M}{\partial H}\tag{9}$$

The specific heat can be expressed as

$$C_V=\frac{d\langle H\rangle}{dT}\tag{10}$$

Therefore the above equations can be solved self-consistently. In the calculations, an initial state, composed of correlation functions, is put into the equations to produce resultant values. The iteration goes on until the convergence is reached.

3. Results and discussion

In the following discussion, J_2 is taken to be an energy unit, and other parameters J_1, J_3 are set in unit of J_2. In this paper, the results are obtained with the anisotropy parameter is set to 0.05. First, we start our analysis with the (J_1, h) phase diagram at zero temperature for $J_3=0.6$, and $J_3=2.0$, respectively. Whether or not J_3 is larger than J_2, Fig. 2(a) and (b) present that both the phase diagrams are composed of five regimes distinguished by four critical lines (labeled h_1, h_2, h_3, and h_4 in the figure), similar to that of the tetrameric ladder-like system [25]. The regimes I, III and V are magnetization plateaus with 0, 1/2 and saturation magnetization plateau (Ms), while the regimes II and IV are gapless phases.

For further visualizing the field dependence of magnetization, the magnetization curves are shown in Fig. 3(a)–(c). Apparently, the appearance of three plateaus satisfies the OYA theory [26]. When J_1 equals J_3, the fourfold magnetic periodic system becomes twofold period, and the 1/2 magnetization plateau disappears, which is shown in Fig. 3(b). While the 1/2 magnetization plateau occurs during the magnetization process for the case that J_1 is not the same as J_3, as depicted in Fig. 3(a) and (c). When J_1 is smaller than J_3, the spin-singlet pairs connected by J_1, J_2 and J_3 are all destroyed, wherein the singlet between 4i+1 and 4i+2 plays the dominate role, which is confirmed by Fig. 3(a). From the figure, it can be seen that the magnetic moments of all the four sites in the unit cell contribute to the 1/2 plateau, yet the m_1 and m_2 win over m_3 and m_4. When J_1 is larger than J_3 (see Fig. 3(c)), the spin-singlet pairs are also destroyed for the 1/2 plateau, wherein the singlet between 4i+3 and 4i+4 is more easily destroyed than the other singlet-pairs, and the m_3 and m_4 win over m_1 and m_2. Fig. 3(d)–(f) plot the h dependence of the two-site entanglement entropy.

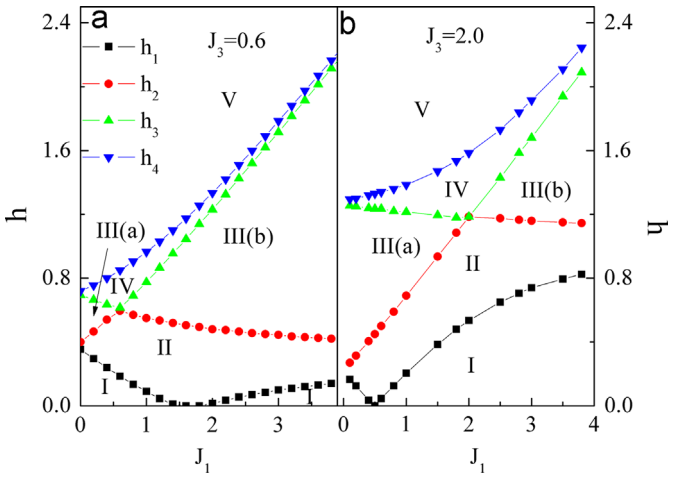

Fig. 2. The (J_1, h) phase diagram for (a) $J_3=0.6$; and (b) $J_3=2.0$.